

# Three-Dimensional Modeling of Tidal Circulation in Bay of Fundy

S. Sankaranarayanan<sup>1</sup> and Deborah French McCay<sup>2</sup>

**Abstract:** A three-dimensional (3D) hydrodynamic model application to the Bay of Fundy was performed using a boundary-fitted coordinate hydrodynamic model. Because the Saint John River and Harbour area were of interest for this study, a very fine grid with a resolution range of 50–100 m was used in the Saint John Harbour region, while a grid resolution of about 2–3 km was used in the Bay of Fundy. The model forcing functions consist of tidal elevations along the open boundary and fresh water flows from the Saint John River. The model-predicted surface elevation compares well with the observed surface elevation at Saint John and the root mean square error in the model-predicted surface elevation for a 60-day period is found to be 4%. The amplitudes and phases of the major tidal constituents at 24 tidal stations, obtained from a harmonic analysis of a 60-day simulation, compares well with the observed data obtained from Canadian Hydrographic Survey. The predicted harmonic amplitudes and phases of the  $M_2$  tidal constituent are, respectively, within 20 cm and 7° of the observed data. The counterclockwise gyre observed in the body of Bay of Fundy is reproduced in the model.

**DOI:** 10.1061/(ASCE)0733-950X(2003)129:3(114)

**CE Database subject headings:** Rivers; Three-dimensional models; Hydrodynamics; Bays; Canada.

## Introduction

The Saint John River originates in the Appalachian Mountains and empties into the Bay of Fundy. A narrow, shallow sill 3–4 m deep demarcates the estuarine and river regimes (Godin 1991). The river widens near the mouth, then passes through the sill to enter Saint John Harbour. Strong tides that enter the sill area through a gorge create a strong current alternating in direction, known as the “Reversing Falls” (Godin 1991). Godin investigated the hydraulics of Saint John River from the observed tidal elevation in the river and suggested that the observed 15- and 28-day oscillations are created by the periodic retention of fresh water during intervals of spring tide. Godin concluded that the increased discharge in the river damps the tide progressing upstream but enhances the 15- and 28-day oscillations. Godin also concluded from the observations that the large tide present at the mouth of the river could not enter the river, which he attributes to the impenetrable barrier caused by the reversing falls.

The world’s highest tides occur in the Bay of Fundy and have been attributed to the fact that the natural period of the Gulf of Maine-Bay of Fundy system is close to the  $M_2$  period of 12.42 h (Greenberg 1979). Greenberg’s (1979) modeling domain included the whole of Bay of Fundy and the Gulf of Maine. Greenberg (1979) also gives a historical review of analytical and simplified model studies in the Bay of Fundy. Greenberg’s (1979) model

included the effects of Coriolis acceleration, real depth, and quadratic bottom friction. The nonlinear convective terms were neglected except in the Minas Channel and Minas Basin. Four basic grid mesh sizes were used to obtain progressively better resolutions from the Gulf of Maine to the Bay of Fundy. Details of the finite difference schemes and methods for joining the grids are given in Greenberg (1976). Greenberg’s calculations were made with a pure  $M_2$  tidal input specified on the open boundary, and the model was calibrated by adjusting the coefficient of friction and depth in the Gulf of Maine to give the best agreement with the analyses of observed tidal elevations at 74 stations in the model domain. Greenberg (1976) concluded that a large part of the mean circulation could be due to tidal rectification modified by meteorological forcing, but he could not confirm this due to the doubts about the appropriate open boundary conditions. Greenberg (1979, 1990) gives a detailed account of modeling studies in the Bay of Fundy and also states that his model does not reproduce the counterclockwise gyres seen in Bay of Fundy.

Isaji and Spaulding (1984) used a 3D numerical model to study the tidally induced residual flows in the Gulf of Maine-Georges Bank region using a 6.25-km square grid. Tidal elevations in terms of  $M_2$  phase and amplitude along the open boundary are specified using the Schwiderski (1979, 1980) deep ocean tidal model. Lynch and Naime (1993) studied the 3D circulation due to  $M_2$  tide and its residual circulation in Gulf of Maine with emphasis on Georges Bank, Browns Bank, Nantucket shoals, and the nearshore region off Cape Sable. Computed  $M_2$  amplitudes of surface elevations and currents were compared with the observed data available in the literature.

## Sources of Available Data for Bay of Fundy and Saint John River

All the previous hydrodynamic modeling studies in the Bay of Fundy (Greenberg 1976, 1979) did not include the Saint John River in their model grid. In the present study, it was decided to

<sup>1</sup>Applied Science Associates, 70, Dean Knauss Dr., Narragansett, RI 02882. E-mail: sankar@appsci.com

<sup>2</sup>Applied Science Associates, 70, Dean Knauss Dr., Narragansett, RI 02882. E-mail: dfrench@appsci.com

Note. Discussion open until October 1, 2003. Separate discussions must be submitted for individual papers. To extend the closing date by one month, a written request must be filed with the ASCE Managing Editor. The manuscript for this paper was submitted for review and possible publication on March 29, 2002; approved on November 6, 2002. This paper is part of the *Journal of Waterway, Port, Coastal, and Ocean Engineering*, Vol. 129, No. 3, May 1, 2003. ©ASCE, ISSN 0733-950X/2003/3-114–123/\$18.00.

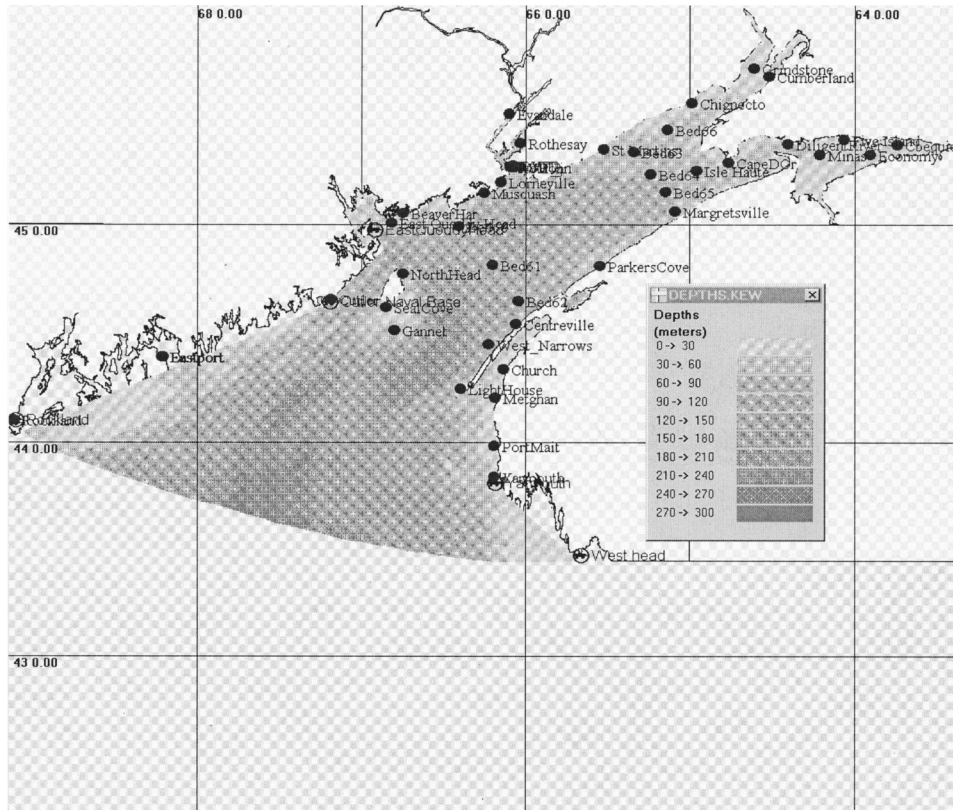


**Fig. 1.** Bay of Fundy bathymetry and station locations

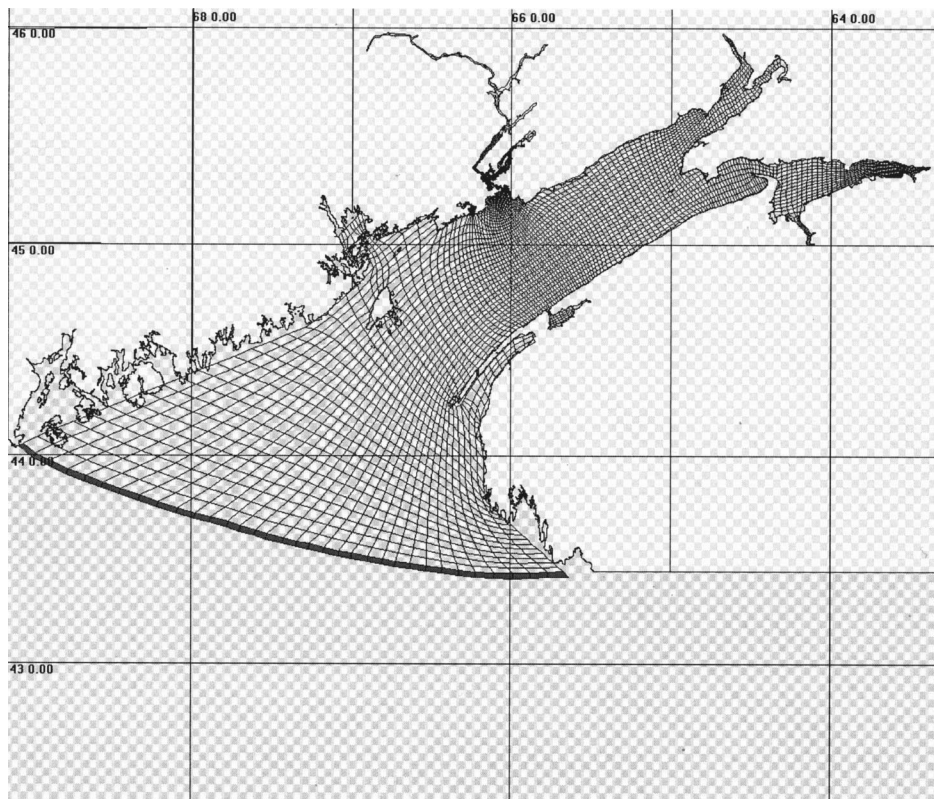


**Fig. 2.** Boundary-fitted grid for the Bay of Fundy



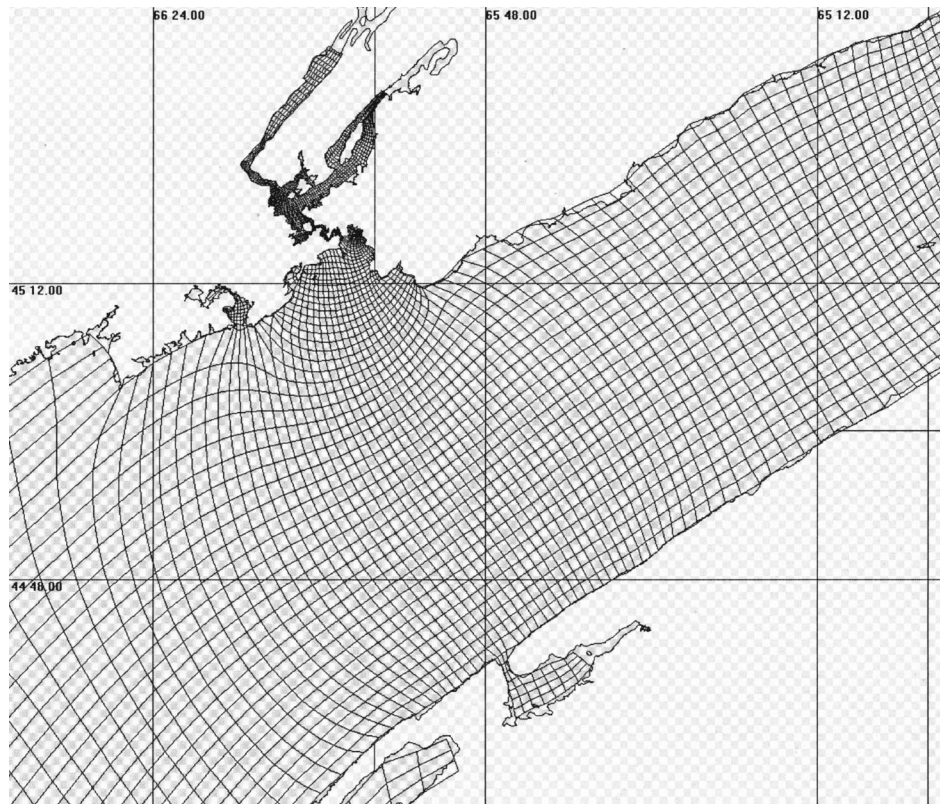


**Fig. 3.** Detail of the boundary-fitted grid in Saint John River region

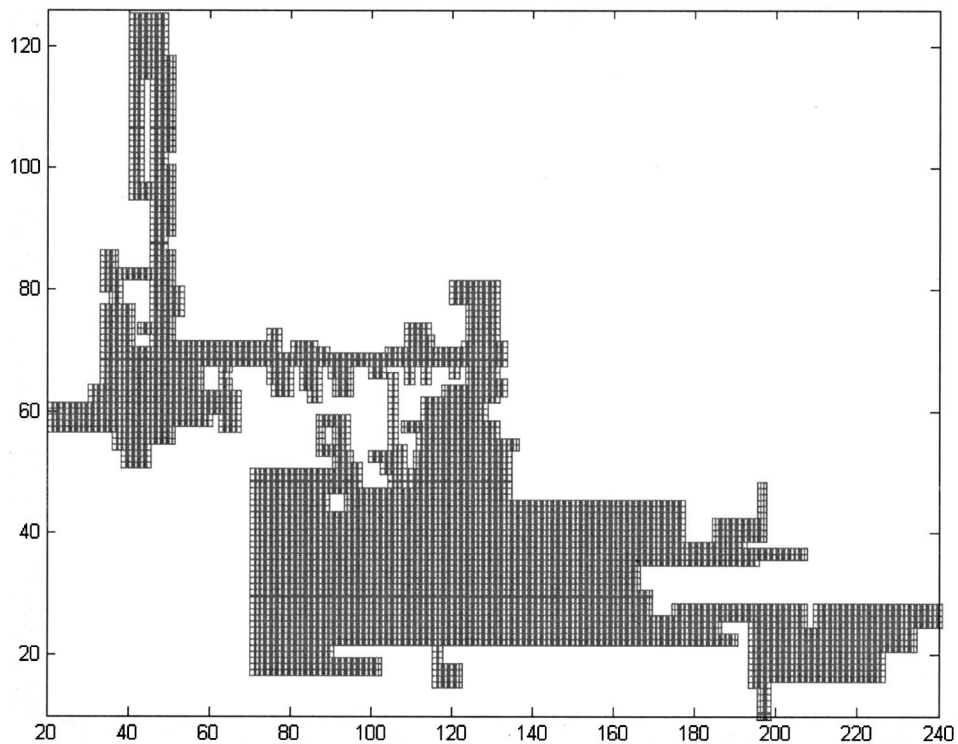


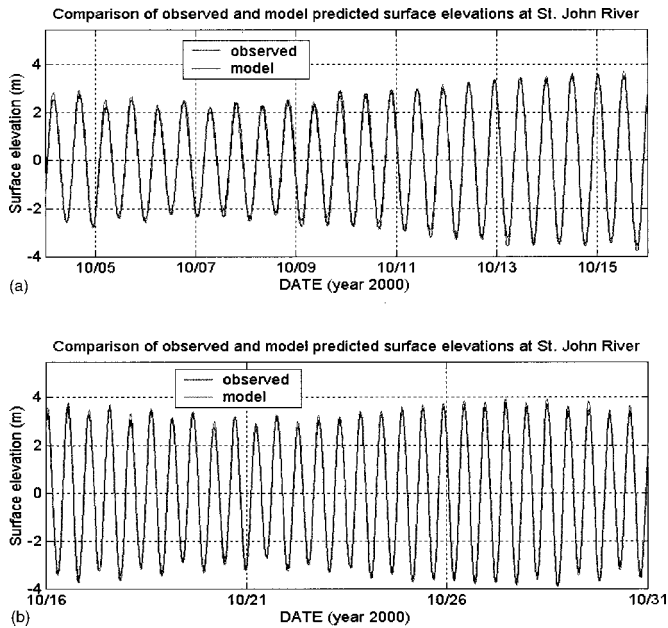
**Fig. 4.** Boundary-fitted grid in the transformed plane

**Table 1.** Range of Grid Angles for Grid

Range of grid angles	Number of grid cell corners
0–30°	10
30–40°	991
40–50°	668
50–60°	938
60–70°	2,723
70–80°	7,452
80–90°	11,730

**Table 2.** Observed Amplitudes and Local Phases of Different Tidal Constituents in West Head and Rockland

Constituent	West Head		Rockland	
	Amp (m)	Phase (°)	Amp (m)	Phase (°)
Z0	1.688	0.0	1.602	0.0
O1	0.105	87.8	0.118	86.6
K1	0.132	105.9	0.152	110.9
M2	1.090	270.9	1.500	283.9
S2	0.216	299.3	0.195	313.2
M4	0.047	265.5	0.000	302.0
N2	0.253	245.2	0.330	254.7
L2	0.025	281.1	0.042	313.2
P1	0.051	105.8	0.051	111.3
2N2	0.006	291.5	0.044	225.3
NU2	0.050	241.1	0.064	258.5
K2	0.000	0.0	0.053	312.6
M6	0.016	317.1	0.035	296.5

**Fig. 5.** Comparison of observed and predicted surface elevations at Saint John Harbour

use a boundary-fitted hydrodynamic model with a very fine grid resolution in the Saint John River (Muin and Spaulding 1997b) to predict the currents in the lower river. High resolution bathymetry for the Saint John River and Musquash Basin was obtained from John Hughes Clarke of the University of New Brunswick. The mean river flows given in Godin (1991) were used as the fresh water flows into the Bay. The observed surface elevations at Saint John Harbour from the Fisheries and Oceans of Canada (available online ([http://www.meds-sdmm.dfo-mpo.gc.ca/alphapro/zmp/slev/saintjohn\\_e.shtml](http://www.meds-sdmm.dfo-mpo.gc.ca/alphapro/zmp/slev/saintjohn_e.shtml))) were used for comparing the model predictions.

### Model Description

The hydrodynamic model used in the present study is a state-of-the-art, 3D, time-dependent, generalized, nonorthogonal,

**Table 3.** Comparison of Observed<sup>a</sup> and Predicted Amplitudes and Greenwich Phase Lags in Bay of Fundy

Station	Observed amplitude (m)	Predicted amplitude (m)	Deviation (m)	Observed phase (°)	Predicted phase (°)	Deviation (°)
West Narrow	2.230	2.305	-0.075	78	78.6	-0.6
Centreville	2.650	2.541	0.109	90	83.6	6.4
Saint John	3.030	3.051	-0.021	98	92.9	5.1
Parkers cove	3.430	3.370	0.060	90	83.6	6.4
Saint Martins	3.690	3.775	-0.085	102	95.5	6.5
Margretnville	3.860	4.050	-0.190	93	87.8	5.2
Isle Haute	4.180	4.320	-0.140	99	92.8	6.2
Chignecto	4.180	4.417	-0.237	103	96.9	6.1
Cape_D_Or	4.340	4.635	-0.295	102	97.3	4.7
Cumberland	4.740	5.051	-0.311	105	101.4	3.6
Grindstone	4.820	5.027	-0.207	105	101.8	3.2
Minas	5.480	5.914	-0.434	121	111.1	9.9
Economy	5.890	6.340	-0.450	126	120.7	5.3
Cbequid	6.060	6.550	-0.490	129	130.5	-1.5

<sup>a</sup>D. A. Greenberg, personal communication, 2001.

**Table 4.** Comparison of Observed (Canadian Hydrographic Survey) and Predicted  $M_2$  Harmonic Amplitudes and Greenwich Local Phases in Bay of Fundy

Station	Observed amplitude (m)	Predicted amplitude (m)	Deviation	Observed phase (°)	Predicted phase (°)	Deviation (°)
Yarmouth	1.658	1.632	0.026	305.6	311.5	-5.9
Port Maitland	1.851	1.680	0.171	309.7	314.1	-4.4
Metghan	2.026	1.891	0.135	316.0	321.4	-5.4
Light House	2.151	1.932	0.219	325.0	323.6	1.4
Church	2.162	1.972	0.190	315.8	321.6	-5.8
Ganet	2.087	2.053	0.034	334.3	329.1	5.2
Seal	2.023	2.211	-0.188	337.3	331.8	5.5
Cutler	1.921	2.031	-0.110	337.2	336.1	1.1
North Head	2.521	2.410	0.111	338.6	335.1	3.5
Centreville	2.650	2.497	0.153	334.4	333.4	1.0
Musquash	2.927	2.795	0.132	342.4	335.2	7.2
Lorneville	3.106	2.930	0.176	342.2	336.5	5.7
Saint John	3.014	3.051	0.021	342.1	338.3	3.8
Parkers Cove	3.434	3.184	0.250	333.9	337.6	-3.7
Saint Martins	3.685	3.678	0.007	345.7	340.5	5.2
Margretnville	3.864	3.846	0.018	337.0	341.2	-4.2
Isle Haute	4.152	4.168	-0.016	343.3	343.4	-0.1
Cape_D_Or	4.340	4.507	-0.167	346.1	346.9	-0.8
Grindstone	4.716	4.871	-0.155	351.1	349.7	1.4
Diligent	4.877	5.426	-0.549	356.5	354.8	1.7

**Table 5.** Comparison of Observed (Canadian Hydrographic Survey) and Predicted  $N_2$  Harmonic Amplitudes and Local Phases in Bay of Fundy

Station	Observed amplitude (m)	Predicted amplitude (m)	deviation (m)	Observed phase (°)	Predicted phase (°)	Deviation (°)
Yarmouth	0.351	0.304	0.047	280.2	296.9	-16.7
Port Maitland	0.387	0.310	0.077	293.3	299.2	-5.9
Metghan	0.426	0.340	0.086	301.1	306.5	-5.4
Light House	0.451	0.346	0.105	297.0	308.8	-11.8
Church	0.425	0.354	0.071	291.1	306.9	-15.8
Ganet	0.463	0.367	0.096	307.3	314.8	-7.5
Cutler	0.422	0.371	0.051	310.8	321.7	-10.9
North Head	0.356	0.435	-0.079	314.4	320.1	-5.7
Centreville	0.658	0.446	0.212	317.6	318.6	-1.0
Musquash	0.603	0.498	0.105	316.8	320.3	-3.5
Lorneville	0.640	0.521	0.119	316.6	321.7	-5.1
Saint John	0.596	0.519	0.077	313.8	323.5	-9.7
Parkers Cove	0.658	0.563	0.095	307.1	322.9	-15.8
Saint Martins	0.903	0.647	0.256	314.6	325.9	-11.3
Margretnville	0.744	0.729	0.015	307.1	329.0	-21.9
Isle Haute	0.910	0.784	0.126	319.5	332.5	-13.0
Cape_D_Or	1.150	0.842	0.308	315.0	336.3	-21.3
Grindstone	1.032	0.934	0.098	327.9	340.7	-12.8
Diligent	1.213	1.033	0.180	351.7	348.0	3.7

**Table 6.** Comparison of Observed (Godin 1991) and Predicted Amplitudes and Local Phases for Different Tidal Constituents in Saint John Harbour

Station	Observed amplitude (m)	Predicted amplitude (m)	Deviation (m)	Observed phase (°)	Predicted phase (°)	Deviation (°)
$M_2$	3.030	3.051	-0.021	342.0	336.9	5.1
$N_2$	0.620	0.506	0.114	313.0	315.8	-2.8
$S_2$	0.495	0.476	0.019	17.0	6.4	10.6
$K_1$	0.153	0.150	0.003	118.1	125.2	-7.1
$O_1$	0.116	0.113	0.003	113.1	118.1	-5.0
$M_4$	0.052	0.023	0.029	170.0	135.6	34.4
$M_6$	0.036	0.034	0.002	341.0	306.2	34.8

boundary-fitted model in spherical coordinates developed by Muin and Spaulding (1997b). The coded application of this model, Boundary Fitted Hydrodynamic model (BFHYDRO) has been successfully applied to coastal and estuarine waters. Some recent applications for the model include the Mount Hope Bay (Swanson et al., 1998) and Providence River (Muin and Spaulding 1997a). The model solves a coupled system of partial differential prognostic equations describing conservation of mass, momentum, salt, and temperature in a generalized, nonorthogonal, boundary-fitted coordinate system. The governing equations in spherical coordinates (Muin and Spaulding 1997a,b) are transformed to a  $\sigma$ -coordinate system in the vertical plane and a generalized nonorthogonal coordinate system in the horizontal plane. The fully transformed equations are given in Muin and Spaulding (1997b). The equations of motion are split into exterior and interior modes to increase the allowable time step and reduce the computational time. Solution of the exterior mode using a semi-implicit solution methodology has been described in Muin and Spaulding (1997b). The vertical diffusion term for the interior mode is solved implicitly using a three-time level scheme. The spatial discretization is based on a space-staggered grid system (Arakawa and Lamb 1977) and the temporal discretization is based on three-level scheme with a weighting factor of 1.5. Thus, the algorithm is second-order in time and space. The boundary-fitted model technique matches the model coordinates with the shoreline boundaries and allows the user to adjust the model grid resolution, as desired. Thus, the system allows the user to use a very fine grid resolution in the Saint John River with the grid closely fitting the river boundaries and a coarse grid resolution in the Bay of Fundy region.

Because tidal circulation is of primary importance in this study, baroclinic effects are neglected. The vertical viscosity  $A_v$  is assumed to be vertically constant and horizontal, and temporal variations are allowed of the form (Davies and Furnes 1980; Lynch and Naimie 1993)  $A_v(\phi, \theta, t) = N_0(\bar{u}^2 + \bar{v}^2)$  where  $(\bar{u}, \bar{v})$  are the vertically averaged velocities in the  $(\phi, \theta)$  directions, respectively, and  $N_0$  is taken to be 0.2 s. At the open boundaries, the water surface elevation is specified as a function of time. At the closed boundaries, the normal velocities are set to zero. The river boundaries are given by a specified inflow-velocity and horizontal pressure gradient set to zero. A time step of 10 min is used for the simulations reported in this study.

### Model Study Area

The model domain along with its bathymetry and tidal station locations are shown in Fig. 1. A 15 arc-s ArcInfo format grid obtained from the Canadian nautical charts was used to generate

the bathymetry for the Bay of Fundy and for the Saint John River. The boundary-fitted grid for the study area is shown in Fig. 2. Details of the grid in the Saint John River are shown in Fig. 3. The grid in Fig. 4 consists of 119×227 segments with 5,952 water cells in the horizontal plane and 10 sigma levels in the vertical plane. Table 1 gives a summary of the number of grid cell corners for various grid angles in those ranges for the boundary-fitted grids used in this study, and a grid angle of 90° represents an orthogonal grid. It is seen that the 93% of the grid cell corners have grid angles greater than 60°. The size of grid cells ranged from 250 m in the river to about 2,500 m in the Bay. Taking the average depths of water to be 40 and 150 m, respectively in the river and the bay, the grid resolution works out to be about 3,500 and 650 grids per wavelength, respectively for the semidiurnal tide. This grid resolution was shown to be adequate to model the tidal circulation (Sankaranarayanan and Spaulding 2003). The bathymetry was mapped onto the boundary-fitted grid. The grid system was designed to provide a good resolution in the Bay of Fundy region and higher resolution in the vicinity of the Saint John River region. The ability of the boundary-fitted grid system to use variable grid lengths in the Bay of Fundy and Saint John River is clearly seen.

### Model Forcing Functions

The 17 major tidal constituents for the tidal stations at West Head and Rockland, located at either end of the open boundary, are given in Table 2. It can be observed from Table 2 that the amplitudes and phases at both ends of the open boundary for the  $M_2$  constituent varies respectively by 0.5 m and 15°. Hence, the tidal harmonics for the cells along the open boundary are obtained from a linear interpolation of the harmonics at West Head and

**Table 7.** Location of Current Measurements (Moody et al. 1984) in Bay of Fundy

Station	Latitude	Longitude	Depth above bottom (m)
Bed 65	45 08 N	65 08 W	37
Bed 66	45 25 N	65 07 W	13
Bed 64	45 13 N	65 14 W	40
Bed 63	45 19 N	65 20 W	25
Bed 62	44 39 N	66 02 W	77
Bed 61	44 49 N	66 12 W	94
Bed 60	45 00 N	66 24 W	71



**Table 8.** Comparison of Observed (Moody et al. 1984) and Predicted  $M_2$  Harmonic Principal Currents

Station	Depth (m)	Principal Current Speed (m/s)		Deviation (m/s)	Orientation of the Principal Current (°)		Deviation (°)
		Observed	Predicted		Observed	Predicted	
Bed61 (surface)	94	0.810	0.785	0.025	72	47.5	24.5
Bed61 (middepth)	57	0.869	0.793	0.076	67	47.5	19.5
Bed62	77	1.091	0.964	0.127	68	48.7	19.3
Bed63	25	0.893	1.047	-0.154	61	57.0	4.0
Bed64 (surface)	40	1.179	1.088	0.091	59	60.7	-1.7
Bed64 (bottom)	25	0.998	1.039	-0.041	59	58.8	0.2
Bed65 (middepth)	37	1.042	1.177	-0.135	52	60.9	-8.9
Bed66 (middepth)	13	0.725	0.927	-0.202	64	53.5	10.5

**Table 9.** Comparison of Observed (Moody et al. 1984) and Predicted  $M_2$  Harmonic Greenwich Phases and Minor Currents

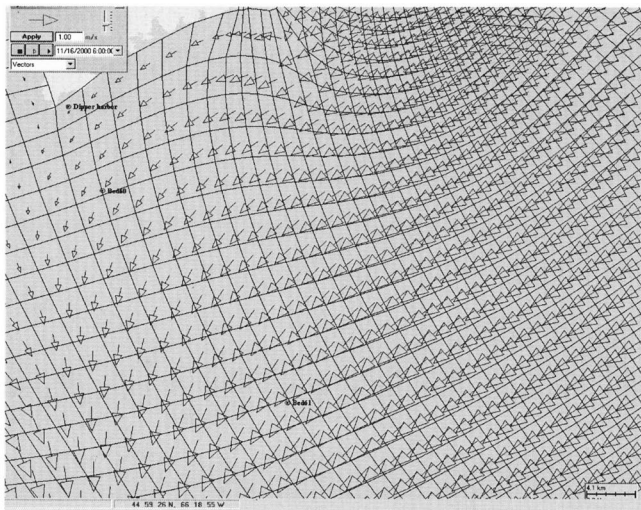
Station	Depth (m)	Minor Current Speed (m/s)		Deviation (m/s)	Phase		Deviation (°)
		Observed	Predicted		Observed	Predicted	
Bed61 (surface)	94	0.072	0.036	0.036	20	16.4	3.6
Bed61 (middepth)	57	0.050	0.037	0.013	15	14.3	0.7
Bed62	77	0.126	0.029	0.097	17	18.0	-1.0
Bed63	25	0.003	-0.009	0.012	20	17.6	2.4
Bed64 (surface)	40	0.099	-0.011	0.110	19	20.1	-1.1
Bed64 (bottom)	25	-0.040	-0.011	-0.029	25	17.3	7.7
Bed65 (middepth)	37	0.013	-0.008	0.021	21	20.8	0.2
Bed66 (middepth)	13	0.097	0.031	0.066	26	16.6	9.4

**Table 10.** Comparison of Observed (Moody et al. 1984) and Predicted  $N_2$  Harmonic Principal Currents

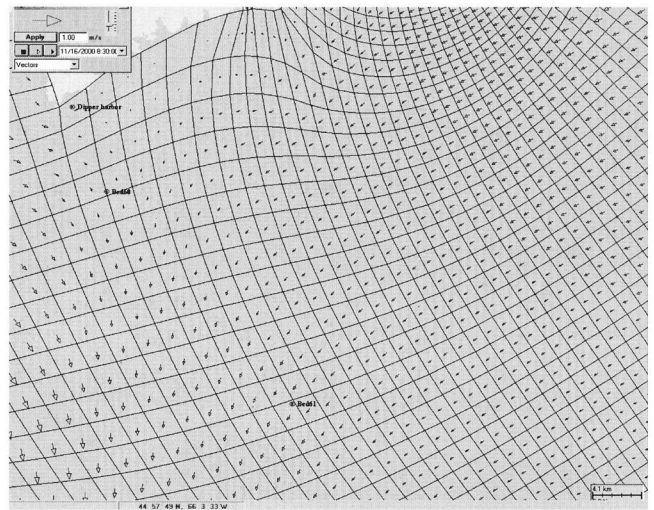
Station	Depth (m)	Principal Current Speed (m/s)		Deviation (m/s)	Orientation of the Principal Current (°)		Deviation (°)
		Observed	Predicted		Observed	Predicted	
Bed61 (surface)	94	0.162	0.136	0.026	64	46.5	17.5
Bed61 (middepth)	57	0.174	0.138	0.036	67	46.7	20.3
Bed62	77	0.218	0.169	0.049	68	48.6	19.4
Bed63	25	0.179	0.178	0.001	59	56.9	2.1
Bed64 (surface)	40	0.236	0.187	0.049	59	60.0	-1.0
Bed64 (bottom)	25	0.199	0.181	0.018	60	58.4	1.6
Bed65 (middepth)	37	0.209	0.212	-0.003	52	60.7	-8.7
Bed66 (middepth)	13	0.145	0.166	-0.021	60	52.6	7.4

**Table 11.** Comparison of Observed (Moody et al. 1984) and Predicted  $N_2$  Harmonic Greenwich Phases and Minor Currents

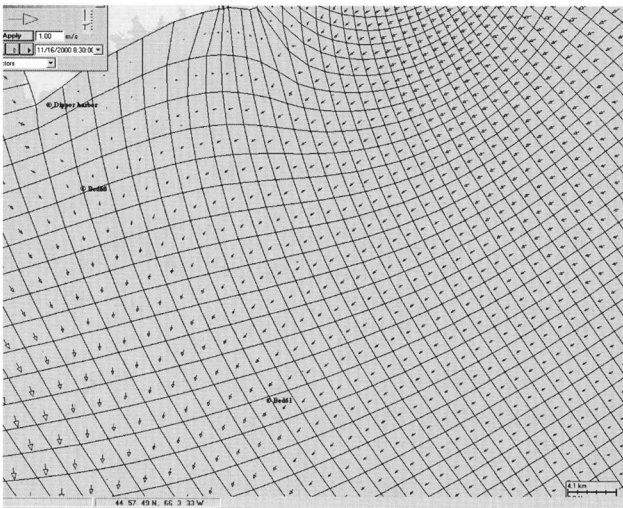
Station	Depth (m)	Minor Current Speed (m/s)		Deviation (m/s)	Phase		Deviation (°)
		Observed	Predicted		Observed	Predicted	
Bed61 (surface)	94	0.019	0.004	0.015	360	359.8	0.2
Bed61 (middepth)	57	0.010	0.008	0.002	350	357.1	-7.1
Bed62	77	0.025	0.004	0.021	351	359.5	-8.5
Bed63	25	0.000	0.002	-0.002	360	1.2	-1.2
Bed64 (surface)	40	0.019	0.004	0.015	354	3.7	-9.7
Bed64 (bottom)	25	0.000	0.006	-0.006	352	1.8	-9.8
Bed65 (middepth)	37	0.030	0.001	0.029	356	6.7	-10.7
Bed66 (middepth)	13	0.005	0.012	-0.007	352	1.7	-9.7



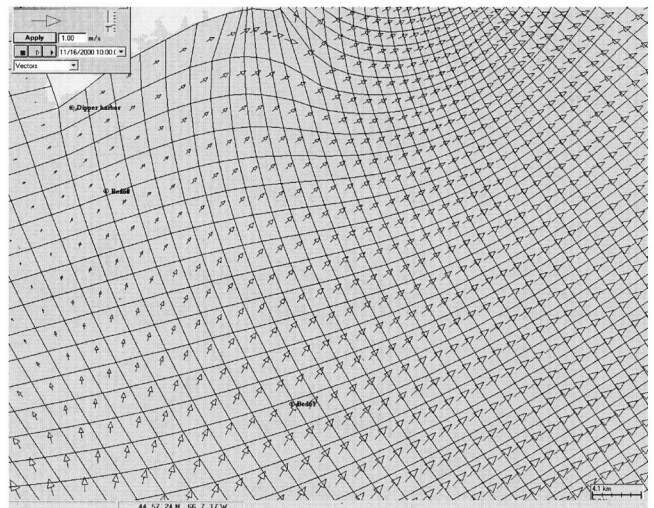
(a)



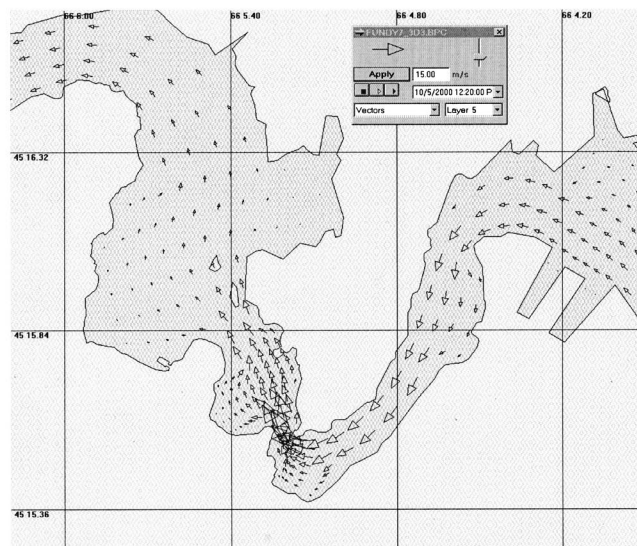
(c)



(b)



(d)



(e)

**Fig. 6.** Model-predicted currents: (a) peak ebb; (b) 2 h after the peak ebb; (c) 3 h after the peak ebb; (d) 4 h after the peak ebb; and (e) hydrodynamic model-predicted flood tide currents in Reversing Falls in Saint John River



Rockland and used as a boundary condition. The mean river flows given in Godin (1991) were used as the fresh water flows into the Bay.

## Model Skill Assessment

Effects of Coriolis acceleration and quadratic bottom friction were included in the model. The surface elevation at Saint John Harbour, available from the Marine Environmental Data Service of the Canada's Department of Fisheries and Oceans (on-line), was used for the model calibration. The model calibration was performed, varying the bottom friction coefficient from 0.001 to 0.005. Comparison of the errors in the model predicted surface elevation with the observed data at Saint John Harbour showed that best results were obtained using a bottom friction coefficient of 0.0010.

## Surface Elevations

The model predicted surface elevation compares well with the observed surface elevations at Saint John Harbour gauging station (Fig. 5), and the RMS error in the model predictions for a 60-day simulation is found to be 4%. Amplitudes and phases of the  $M_2$  harmonic tidal constituent in the Bay of Fundy obtained from Greenberg (2001, personal communication) were also used for model comparison. Errors in the computed amplitudes and phases of the  $M_2$  tidal constituent are compared in Table 3. It can be seen that the amplitudes are within 20 cm for most stations, except for those in the upper Bay of Fundy. The highest error in amplitude of 50 cm is found to occur at Cbequid in the upper Bay for an observed amplitude of 6.06 m. The Greenwich phases for most stations are within  $7^\circ$  of the observed data, except at Minas Basin in the upper Bay. Additional data for  $M_2$  and  $N_2$  harmonic tidal constituents at 22 stations obtained from Canadian Hydrographic Survey (CHS) are also used to compare the model predicted harmonic constituents. The errors in predicted amplitudes are found to be within 10%, and the maximum errors for the phases are found to be less than  $7^\circ$  (Table 4). The errors in the computed amplitudes and phases (Table 5) for the  $N_2$  constituent are higher. However their magnitudes are relatively small, when compared with that of the  $M_2$ . A comparison of the observed and predicted amplitudes and local phases (Atlantic Time Greenwich Mean Time—04:00) at Saint John Harbour for 7 tidal constituents (Godin 1991) is shown in Table 6. The error in the predicted  $M_2$  amplitude at Saint John Harbour is 3 cm and the error in the phase is about  $5^\circ$ , which translates into a time lag of 10 min between the observations and predictions. The errors in the predicted amplitudes and phases for the other constituents are higher, but their magnitudes are relatively small when compared with  $M_2$ .

## Harmonic Currents

The model-predicted harmonic principal currents, directions, and phases at eight locations (Table 7) for the  $M_2$  and  $N_2$  harmonic constituents are compared with those reported in *U.S. Geological Survey Bulletin* 1611 (Moody et al. 1984). The error in the principal current speeds (Tables 8–11) are found to be within 10% except at station Bed 66 and the error in the directions are within  $10^\circ$  except at stations Bed 61 and Bed 62 (Table 8). The errors in principal current phases are within  $20^\circ$  at all stations (Table 9). The errors in the principal current magnitudes are found to be within 20% at all stations and the errors in the directions are

within  $10^\circ$ , except at stations Bed 61 and Bed 62 (Table 10). The errors in the principal current phases are within  $10^\circ$  at all stations. The vertical structure of the current is found to be constant, except in the River. Very strong currents of the order of 10 m/s are found to develop in the River, and a very prominent vertical current structure is seen in the River. The model predictions of currents in the River could not be compared with observations due to lack of data. A counterclockwise gyre, observed in the Bay of Fundy, was reproduced in the model as shown in Figs. 6(a–d). Fig. 6(e) shows the model predicted flood tide currents in Reversing Falls in the Saint John River.

## Conclusions

The model-predicted, tidal surface elevations compare well with those observed at Saint John Harbour, and the RMS error of the model predictions is found to be less than 4%. The errors in the model predicted amplitudes of the  $M_2$  harmonic tidal constituent at 22 stations are within 0.2 m, and the errors in the phases are within  $7^\circ$ , except for stations in the upper Bay. The amplitudes and phases for the  $N_2$  harmonic tidal constituent compare favorably with the observations. The vertical structure of the model-predicted harmonic current compares well with the observations.

## Acknowledgments

The writers thank Canadian Hydrographic Survey for providing us the observed tidal constituent data in the Bay of Fundy. Valuable insights provided by David Greenberg, Bedford Institute of Oceanography and Daniel Mendelsohn of ATM are also very much appreciated. They also thank Hughes Clarke, University of New Brunswick, for providing us the fine resolution bathymetry for the Saint John River and Musquash Basins. This work was funded in part by New Brunswick Power through Golder Associates, Gainesville, Fla. office, with Isabel Johnson serving as the project manager.

## References

- Arakawa, A., and Lamb, V. R. (1977). "Computational design of the basic dynamical processes of the ULCA General Circulation Model." *Methods Comput. Phys.*, 17, 173–265.
- Davies, A. M., and Furnes, G. K. (1980). "Observed and computed  $M_2$  tidal currents in the North Sea." *J. Phys. Oceanogr.*, 10, 237–257.
- Godin, G. (1991). "Tidal hydraulics of Saint John River." *J. Waterw., Port, Coastal, Ocean Eng.*, 117(1), 19–28.
- Greenberg, D. A., (1976). "Numerical studies of tidal behavior in Bay of Fundy." PhD thesis, University of Liverpool, Liverpool, U.K.
- Greenberg, D. A. (1979). "A numerical model investigation of tidal phenomena in the Bay of Fundy and Gulf of Maine." *Marine Geodesy*, 2, 161–187.
- Greenberg, D. A. (1990). "The contribution of modeling to understanding the dynamics of the Bay of Fundy and Gulf of Maine." *Modeling marine systems*, Vol. 2, A. M. Davies, ed., CRC Press, Boca Raton, Fla., 107–140.
- Isaji, T., and Spaulding, M. L. (1984). "Model of the tidally induced residual circulation in the Gulf of Maine and Georges Bank." *J. Phys. Oceanogr.*, 14, 1119–1126.
- Lynch, D. R., and Naimie, C. R. (1993). "The  $M_2$  tide and its residual on the outer banks of the Gulf of Maine." *J. Phys. Oceanogr.*, 23(10), 2222–2253.

- Moody, J. A. et al. (1984). "Atlas of tidal elevation and current observations on the Northeast American continental shelf and slope." *U.S. Geol. Surv. Bull.*, 1611.
- Muin, M., and Spaulding, M. L. (1997a). "Application of three-dimensional boundary-fitted circulation model to Providence River." *J. Hydraul. Eng.*, 123(1), 13–20.
- Muin, M., and Spaulding, M. L. (1997b). "Three-dimensional boundary-fitted circulation model." *J. Hydraul. Eng.*, 123(1), 2–12.
- Sankaranarayanan, S., and Spaulding, M. L. (2003). "A study of the effects of grid nonorthogonality on the solution of shallow water equations in boundary-fitted coordinate systems." *J. Comput. Phys.*, 184(1), 299–320.
- Schwiderski, E. W. (1979). "Ocean tides II: A hydrodynamic interpolation model." *J. Marine Geodesy*, 3, 219–255.
- Schwiderski, E. W. (1980). "On charting global ocean tides." *Rev. Geophys. Space Phys.*, 18, 243–268.
- Swanson, J. C., Mendelsohn, D., Rines, J., and Schuttenberg, H. (1998). "Mt. Hope Bay hydrodynamic model calibration and confirmation." *ASA Project Rep. 96-076*, Applied Science Associates, Narragansett, R.I.